

## Magnetic anisotropy barrier for spin tunneling in $\text{Mn}_{12}\text{O}_{12}$ molecules

M. R. Pederson

*Center for Computational Materials Science-6392, Naval Research Laboratory, Washington, D.C. 20375-5000*

S. N. Khanna

*Department of Physics, Virginia Commonwealth University, Richmond, Virginia 23284-2000*

(Received 4 March 1999; revised manuscript received 21 June 1999)

Electronic structure calculations on the nature of electronic states and the magnetic coupling in Mn-acetate [ $\text{Mn}_{12}\text{O}_{12}(\text{RCOO})_{16}(\text{H}_2\text{O})_4$ ] molecules have been carried out within the generalized gradient approximation to the density functional formalism. Our studies on this 100-atom molecule illustrate the role of the nonmagnetic carboxyl host in stabilizing the ferrimagnetic  $\text{Mn}_{12}\text{O}_{12}$  core and provide estimates of the local magnetic moment at the various sites. We provide a first density-functional-based prediction of the second-order magnetic anisotropy energy of this system. Results are in excellent agreement with experiment. To perform these calculations we introduce a simplified exact method for spin-orbit coupling and magnetic anisotropy energies in multicenter systems. This method is free of shape approximations and has other advantages as well. First, it is valid for periodic boundary conditions or finite systems and is independent of basis set choice. Second, the method does not require the calculation of electric field. Third, for applications to systems with a finite energy gap between occupied and unoccupied electronic states, a perturbative expansion allows for a simple determination of the magnetic anisotropy energy. [S0163-1829(99)04437-9]

### I. INTRODUCTION

The magnetic anisotropy energy, first explained by Van Vleck,<sup>1,2</sup> represents a very important energy scale for the design of molecular scale magnetic memory devices. It determines the temperature at which thermal processes will cause the spin projection of a molecule or cluster to randomly reorientate itself. Further, the magnetic fields at which resonant spin tunneling is achieved is related to the anisotropy energy and this relationship is especially simple for uniaxial systems where the barrier is dominated by second-order effects. An example of current interest is the recent observation of resonant quantum tunneling of magnetization (QTM) in  $\text{Mn}_{12}\text{O}_{12}$ -acetate crystals. This observation has generated considerable excitement as it illustrates quantum phenomenon at a macroscopic scale.<sup>3-13</sup> The crystal, first discovered by Lis,<sup>3</sup> consists of  $\text{Mn}_{12}\text{O}_{12}(\text{RCOO})_{16}(\text{H}_2\text{O})_4$  molecules with  $R = \text{CH}_3$  and six additional molecules of solvation (four water and two acetic acid molecules). The unit cell has a volume of 3716 Å<sup>3</sup> and its core is made of a  $\text{Mn}_{12}\text{O}_{12}$  cluster which is ferrimagnetic with a total spin  $S$  of 10 (moment of  $20.0\mu_B$ ). The magnetic  $\text{Mn}_{12}\text{O}_{12}$  clusters in different cells are separated by the nonmagnetic host which prevents any exchange coupling between individual clusters. [The dipolar interaction between neighboring clusters which are separated by 15 Å is estimated to be around 0.01 T (Ref. 5) which is two orders of magnitude smaller than the magnetic fields used in experiments.] Further, the crystal is marked by a uniaxial magnetic anisotropy which results in the energy depending on the orientation of the spin relative to the symmetry axis. Upon application of a magnetic field, hysteresis loops have shown a staircase structure proposed to be associated with resonant quantum tunneling of spins between the different  $M$  states. Based on the Arrhenius behavior of the relaxation times, the total anisotropy barrier has

been estimated to be in the range of 60–62 K.<sup>7</sup> Recently, Barra *et al.*<sup>12</sup> have analyzed the high-field electron paramagnetic resonance data and suggested that the second-order contributions to the anisotropy energy account for 55.6 K of the barrier. Fort *et al.*<sup>13</sup> have performed a detailed analysis on measurements from both activated and tunneling transitions and have found that this second-order contribution plus two additional fourth-order contributions account for the field dependence of the relaxation time.

To date, the only available theoretical electronic structure studies are based on an isolated  $\text{Mn}_{12}\text{O}_{12}$  cluster<sup>14</sup> with the bulk geometry. We have shown<sup>15</sup> that a free  $\text{Mn}_{12}\text{O}_{12}$  cluster with the same geometry as in bulk acetate is unstable and transforms to the Ziemann-Castleman tower structure proposed for free MnO clusters in beams.<sup>16</sup> Our studies also demonstrated that the nonmagnetic host, consisting of sixteen carboxyl groups and four  $\text{H}_2\text{O}$  molecules, performs a key role in stabilizing the magnetic core and in determining the local magnetic moments at the Mn sites. However, there have been no first-principles predictions or explanations dealing with the large second-order contributions to the anisotropy energies. In this paper we present a detailed electronic structure of the molecule. We examine the magnetic structure of the passivated  $\text{Mn}_{12}\text{O}_{12}$  clusters and the states involved in the spin tunneling. The calculated electronic states are used to carry out the first *ab initio* calculation of the magnetic anisotropic energy of this passivated nanomagnet.

In Sec. II we introduce a simplified albeit exact method for incorporating spin-orbit coupling into density-functional calculations and in Sec. III we derive the necessary equations for determining the magnetic anisotropy barrier in a uniaxial system such as the  $\text{Mn}_{12}$ -acetate molecule. The method introduced here is independent of the type of basis set that is employed and is applicable to both isolated and periodic sys-

tems. Further it has several numerical and computational advantages over the standard  $\mathbf{L} \cdot \mathbf{S}$  representation for spin-orbit coupling. It relies on the original Cartesian representation for the spin-orbit coupling interaction but with a simple integration by parts we alleviate the need for the determination of the electric field. To make contact with the spin-tunneling experiments we consider the problem of a uniaxial molecule in a magnetic field and write down the expressions that are needed to calculate the anisotropy energy. In Sec. IV we briefly outline the method used for determining the magnetic ordering, equilibrium geometries, Kohn-Sham orbitals and densities of states. In Sec. V, we present our all-electron density-functional based calculations on the magnetic anisotropy energy for the  $\text{Mn}_{12}$ -acetate molecule and compare our results to the experimental values. A summary follows in Sec. VI.

## II. A SIMPLE EXACT FULL-SPACE APPROACH TO SPIN-ORBIT COUPLING

To date, calculations of spin-orbit coupling have used a generalization of the standard spin-orbit coupling terms for spherical systems. This standard  $\mathbf{L} \cdot \mathbf{S}$  representation for the spin-orbit coupling requires the determination of the electric field observed by the moving electrons and is not entirely straightforward to use in applications to nonspherical or multicenter systems.

The classical explanation of spin-orbit coupling is that an electron moving, with velocity  $\mathbf{v}$ , in an external electric field ( $\mathbf{E}$ ), observes a magnetic field given by  $\mathbf{v} \times \mathbf{E}/c$ . To determine the quantum-mechanical operator within a Hartree approximation it is common to note that  $\mathbf{E} = -\nabla\Phi(\mathbf{r})$ , with  $\Phi$  the Coulomb potential and to replace the velocity ( $\mathbf{v}$ ) by the momentum operator  $\mathbf{p}$ . Accounting for the fact that the electron is not spinless, the interaction energy is then given by<sup>17</sup>

$$U(\mathbf{r}, \mathbf{p}, \mathbf{S}) = -\frac{1}{2c^2} \mathbf{S} \cdot \mathbf{p} \times \nabla\Phi(\mathbf{r}), \quad (1)$$

where the factor of 2 in the denominator, also derivable from the Dirac equation, is due to the Thomas precession. Given a spherically symmetric potential  $\Phi(r)$  and some simple algebraic reductions the above expression is usually rewritten according to

$$U(r, \mathbf{L}, \mathbf{S}) = \frac{1}{2c^2} \mathbf{S} \cdot \mathbf{L} \frac{1}{r} \frac{d\Phi(r)}{dr}. \quad (2)$$

While the above equation is exact for spherical systems, an attempt to approximate the spin-orbit coupling in multicenter systems as a superposition of such terms on a lattice could omit nonspherical corrections that may be especially important for anisotropy energies.

Instead of using Eq. (2) for the spin-orbit coupling we return to Eq. (1) and note that in all basis-set oriented mean-field approaches the single-electron wave functions are ultimately expressed according to

$$\psi_{is}(\mathbf{r}) = \sum_{j\sigma} C_{j\sigma}^{is} f_j(\mathbf{r}) \chi_\sigma, \quad (3)$$

where  $f_j(\mathbf{r})$  is a spatial basis function,  $\chi_\sigma$  is either a majority or minority spin spinor, and the  $C_{j\sigma}^{is}$  are determined by di-

agonalizing (or effectively diagonalizing) the Hamiltonian matrix. In the above equation, we allow for the possibility of noncollinear magnetic wave functions. Regardless of whether one is working with the Dirac equation, a scalar relativistic methodology or nonrelativistic formulations the determination of spin-orbit coupling matrix elements is a necessary ingredient to the numerical solution of the Schrödinger equation. To determine the generalized spin-orbit interaction from Eq. (1) it is simply necessary to calculate matrix elements of the form

$$\begin{aligned} U_{j\sigma, k\sigma'} &= \langle f_j \chi_\sigma | U(\mathbf{r}, \mathbf{p}, \mathbf{S}) | f_k \chi_{\sigma'} \rangle \\ &= \sum_x \frac{-1}{i2c^2} \langle f_j | [\nabla \times \nabla\Phi(\mathbf{r})]_x | f_k \rangle \langle \chi_\sigma | S_x | \chi_{\sigma'} \rangle \\ &= \sum_x \frac{1}{i} \langle f_j | V_x | f_k \rangle \langle \chi_\sigma | S_x | \chi_{\sigma'} \rangle \end{aligned} \quad (4)$$

with the operator  $V_x$  defined according to

$$\begin{aligned} \langle f_i | V_x | f_j \rangle &= \frac{-1}{2c^2} \left\langle f_i \left| \frac{d}{dy} \frac{d\Phi}{dz} - \frac{d}{dz} \frac{d\Phi}{dy} \right| f_j \right\rangle \\ &= \frac{1}{2c^2} \left[ \left\langle f_i \left| \left( \frac{d\Phi}{dy} \frac{d}{dz} - \frac{d\Phi}{dz} \frac{d}{dy} \right) \right| f_j \right\rangle \right. \\ &\quad \left. + \left\langle f_i \left| \frac{d^2\Phi}{dydz} - \frac{d^2\Phi}{dzdy} \right| f_j \right\rangle \right] \\ &= \frac{1}{2c^2} \left\langle f_i \left| \left( \frac{d\Phi}{dy} \frac{d}{dz} - \frac{d\Phi}{dz} \frac{d}{dy} \right) \right| f_j \right\rangle. \end{aligned} \quad (5)$$

We note that if one rewrites Eq. (1) as  $U(\mathbf{r}, \mathbf{p}, \mathbf{S}) = (1/2c^2) \mathbf{S} \cdot \nabla\Phi(\mathbf{r}) \times \mathbf{p}$  we obtain the same final expression for Eq. (5). The most straightforward path to deriving Eq. (5) is to follow Kittel<sup>18</sup> and rewrite the spin-orbit interaction as  $U(\mathbf{r}, \mathbf{p}, \mathbf{S}) = (1/2c^2) \mathbf{S} \times \nabla\Phi(\mathbf{r}) \cdot \mathbf{p}$ . The important point is that all possible classical definitions of the spin-orbit term will eventually lead to Eq. (5). Now using the identity

$$\begin{aligned} \left\langle f_i \left| \frac{d\Phi}{dy} \frac{d}{dz} \right| f_j \right\rangle &= \int d^3r \frac{d}{dy} \left[ f_i \Phi \frac{df_j}{dz} \right] \\ &\quad - \left\langle \frac{df_i}{dy} \left| \Phi \right| \frac{df_j}{dz} \right\rangle - \left\langle f_i \left| \Phi \right| \frac{d^2f_j}{dzdy} \right\rangle \end{aligned} \quad (6)$$

and a similar identity for the  $\langle f_i | (d\Phi/dz)(d/dy) | f_j \rangle$  term of Eq. (5) allows for the introduction of a simple expression for the spin-orbit coupling matrix elements

$$\langle f_i | V_x | f_j \rangle = \frac{1}{2c^2} \left( \left\langle \frac{df_i}{dz} \left| \Phi \right| \frac{df_j}{dy} \right\rangle - \left\langle \frac{df_i}{dy} \left| \Phi \right| \frac{df_j}{dz} \right\rangle \right). \quad (7)$$

The matrix elements for  $V_y$  and  $V_z$  are determined from cyclical permutations of the coordinate labels in the above equation. The above equation follows because the first term of Eq. (6) vanishes if the system is finite since the basis functions vanish at infinity and the third term of Eq. (6) is exactly cancelled by the third term of  $\langle f_i | (d\Phi/dz)(d/dy) | f_j \rangle$ . Equation (7) is also appropriate for periodic

systems since it is only necessary to evaluate the spin-orbit coupling terms between states associated with the same point in the Brillouin zone.<sup>18</sup> Therefore, for a periodic calculation we are only interested in evaluating Eq. (6) for functions with the same  $k$  vector. For functions with the same  $k$  vector the first term of Eq. (6) vanishes because the surface terms cancel one another.

The above representation [Eq. (7)] for the spin-orbit coupling matrix offers several advantages over the more usual representation in terms of Eq. (2). First, it does not require the determination of the electric field and depends only on the ability to accurately determine the Coulomb potential and the gradient of each basis function in the problem. This representation for the spin orbit coupling matrix is especially ideal for basis functions constructed from Gaussian-type orbitals, Slater-type functions, and plane waves. For numerical basis functions it should still be useful since it is generally necessary to determine the gradient of a numerical function for determination of the kinetic energy matrix. Before turning to many-electron systems, where second order effects are of primary interest, the veracity of Eq. (7) can be simply tested by calculating the spin-orbit splitting of the  $2p$  states in the hydrogen atom. It is easily verified that Eq. (4) combined with Eq. (7) predicts the exact first-order splitting of  $1/32c^2$  between the  $^2P_{3/2}$  and  $^2P_{1/2}$  states.<sup>17</sup>

### III. CALCULATION OF MAGNETIC ANISOTROPY ENERGIES

Especially in uniaxial systems the magnetic anisotropy energy is primarily due to spin-orbit coupling and is typically on the order of microhartrees. For systems with a vanishing energy gap between the occupied and unoccupied electronic states, spin-orbit interactions can either rearrange the occupied and unoccupied manifold or possibly open up small gaps. For systems with a finite energy gap such as insulators or nanoscale molecules and clusters, spin-orbit coupling will shift each occupied and unoccupied eigenvalue by  $O(1/2c^2)$  but will generally not cause energy crossings between occupied and unoccupied states. For such systems the anisotropy barrier is related to the shift of the *total energy* as a function of quantization axis rather than the single-electron energies. By making use of a perturbative expansion we show that for closed shell systems the first-order  $O(1/2c^2)$  effects due to spin orbit coupling vanish and it is the second order  $O(1/4c^4)$  effects which account for the shift in total energies, the formation of magnetic anisotropy energies, and other collective effects. We also develop a two-dimensional spin Hamiltonian, which when solved self-consistently, determines the stationary spin orientations as a function of geometry and magnetic-field orientation. A perturbative method for the determination of single-electron and collective shifts in total energies due to spin-orbit coupling is now outlined. We include effects due to magnetic fields as well to make contact with the spin-tunneling experiments. Let us assume that, in the absence of a magnetic field and spin-orbit coupling, we have determined the wave functions  $[\psi_{i\sigma}]$  within a self-consistent field (SCF) approximation (e.g., density-functional theory or Hartree-Fock). The SCF wave functions satisfy

$$H|\psi_{i\sigma}\rangle = \epsilon_{i\sigma}|\psi_{i\sigma}\rangle, \quad (8)$$

where the spin-orbital  $|\psi_{i\sigma}\rangle$  is a simple product of a spatial function and spinor according to  $|\psi_{i\sigma}\rangle = \phi_{i\sigma}(\mathbf{r})\chi_{\sigma}$ . With the inclusion of spin-orbit coupling and the introduction of a magnetic field the perturbed wave functions must satisfy

$$\left[ H + \left( \frac{\mathbf{V}}{i} + \frac{1}{c}\mathbf{B} \right) \cdot \mathbf{S} \right] |\psi'_{i\sigma}\rangle = \epsilon'_{i\sigma} |\psi'_{i\sigma}\rangle \quad (9)$$

with the operator  $\mathbf{V}$  defined according to Eqs. (7) and the magnetic field ( $\mathbf{B}$ ) is assumed to be uniform. If we take  $\mathbf{W} = (\mathbf{V}/i + \mathbf{B}/c)$ , second order perturbation theory tells us that trace of the Hamiltonian matrix is perturbed according to the following expression:

$$\Delta = \Delta_1 + \Delta_2, \quad (10)$$

$$\Delta_1 = \sum_{x\sigma} S_x^{\sigma\sigma} \sum_i \langle \phi_{i\sigma} | W_x | \phi_{i\sigma} \rangle,$$

$$\Delta_2 = \sum_{\sigma\sigma'} \sum_{xy} W_{xy}^{\sigma\sigma'} S_x^{\sigma\sigma'} S_y^{\sigma'\sigma},$$

$$W_{xy}^{\sigma\sigma'} = W_{yx}^{\sigma\sigma'} * = \sum_{ij} \frac{\langle \phi_{i\sigma} | W_x | \phi_{j\sigma'} \rangle \langle \phi_{j\sigma'} | W_y | \phi_{i\sigma} \rangle}{\epsilon_{i\sigma} - \epsilon_{j\sigma'}},$$

$$S_x^{\sigma\sigma'} = \langle \chi_{\sigma} | S_x | \chi_{\sigma'} \rangle. \quad (11)$$

In the above equation the  $\phi_{i\sigma}$  are occupied states and the  $\phi_{j\sigma}$  are unoccupied states. The above equation follows because it is only necessary to determine the first order mixing coefficients between the occupied and unoccupied orbitals to determine the first and second order changes of the trace of the Hamiltonian.

The above expression is valid for any set of spinors ( $\chi_1, \chi_2$ ) which are constructed from a unitary transformation on the  $S_z$  eigenstates ( $\mu_1, \mu_2$ ) defined with respect to an arbitrary axis.

$$|\chi_1\rangle = u_{11}|\mu_1\rangle + u_{12}|\mu_2\rangle,$$

$$|\chi_2\rangle = u_{21}|\mu_1\rangle + u_{22}|\mu_2\rangle. \quad (12)$$

In terms of the unitary matrix the total energy shift ( $\Delta$ ) can then be rewritten according to

$$\Delta = \sum_{\sigma\mu\mu'} u_{\sigma\mu}^* u_{\sigma\mu'} T_{\mu,\mu'}^{\sigma} + \sum_{\sigma\sigma' \mu\mu' \mu'' \mu'''} u_{\sigma\mu}^* u_{\sigma\mu'} u_{\sigma' \mu''}^* u_{\sigma' \mu'''} V_{\mu\mu' \mu'' \mu'''}^{\sigma\sigma'} \quad (13)$$

with the  $T$  and  $V$  matrices defined in terms of the  $W$  matrices according to

$$T_{\mu,\mu'}^{\sigma} = \sum_x \langle \mu | S_x | \mu' \rangle \sum_i \langle \phi_{i\sigma} | W_x | \phi_{i\sigma} \rangle, \quad (14)$$

$$V_{\mu\mu' \mu'' \mu'''}^{\sigma\sigma'} = \sum_{xy} W_{xy}^{\sigma\sigma'} \langle \mu | S_x | \mu'' \rangle \langle \mu'' | S_y | \mu' \rangle. \quad (15)$$

For the most general uniform magnetic field and a system with no symmetry the above equations allow us to find the

groundstate of a molecule as a function of quantization axis. This is accomplished by finding the optimal unitary transformation that lead to stationary values of Eq. (13). One approach to the generalized problem is to introduce Lagrange multipliers to maintain the orthonormality of the vectors ( $\mathbf{u}_1, \mathbf{u}_2$ ) and self-consistently minimize Eq. (13) using standard techniques. An alternative approach, applicable to uniaxial systems, is to parametrize a  $2 \times 2$  unitary transformation in terms of two angles and minimize the above expression as a function of these two angles. We discuss the latter approach within the context of the calculation of the magnetic-anisotropy barriers in molecules.

We now turn to the case of a closed-shell molecule with  $\Delta N$  excess majority spin electrons which exists in a uniaxial symmetry state. Since  $\sum_i \phi_{i\sigma}^*(\mathbf{r}) \phi_{i\sigma}(\mathbf{r}')$  and  $\sum_{ij} \phi_{i\sigma}^*(\mathbf{r}) \phi_{j\sigma'}(\mathbf{r}) \phi_{j\sigma'}^*(\mathbf{r}') \phi_{i\sigma}(\mathbf{r}') / (\epsilon_{i\sigma} - \epsilon_{j\sigma'})$  are invariant under the symmetry operations the first order and second order shifts are significantly simplified. The spin-orbit contributions to the first-order energy shift  $\Delta_1$  sum to zero which leads to a first order contribution written according to

$$\begin{aligned} \Delta_1 &= \sum_{\sigma} \frac{\mathbf{B}}{c} \langle \chi_{\sigma} | \mathbf{S} | \chi_{\sigma} \rangle \times \left[ \sum_i \langle \phi_{i\sigma} | \phi_{i\sigma} \rangle \right] \\ &= \frac{\mathbf{B}}{c} \sum_{\sigma} \langle \chi_{\sigma} | \mathbf{S} | \chi_{\sigma} \rangle \times N_{\sigma}. \end{aligned} \quad (16)$$

With respect to second order shifts the  $W$  matrices are simplified to

$$\begin{aligned} W_{xy}^{\sigma\sigma'} &= - \sum_{ij} \frac{\langle \phi_{i\sigma} | V_x | \phi_{j\sigma'} \rangle \langle \phi_{j\sigma'} | V_y | \phi_{i\sigma} \rangle}{\epsilon_{i\sigma} - \epsilon_{j\sigma'}} \\ &+ \frac{B_x B_y}{c^2} \sum_{ij} \frac{\langle \phi_{i\sigma} | \phi_{j\sigma'} \rangle \langle \phi_{j\sigma'} | \phi_{i\sigma} \rangle}{\epsilon_{i\sigma} - \epsilon_{j\sigma'}}. \end{aligned} \quad (17)$$

The second term of the above expression is responsible for the magnetic susceptibility of the system and is not of primary interest to magnetic anisotropy barriers. At zero or very small fields the  $W$  matrices simplify to

$$W_{xy}^{\sigma\sigma'} \rightarrow M_{xy}^{\sigma\sigma'} = - \sum_{ij} \frac{\langle \phi_{i\sigma} | V_x | \phi_{j\sigma'} \rangle \langle \phi_{j\sigma'} | V_y | \phi_{i\sigma} \rangle}{\epsilon_{i\sigma} - \epsilon_{j\sigma'}}. \quad (18)$$

For uniaxial symmetry the Cartesian off-diagonal  $M$  matrices vanish and  $M_{xx}^{\sigma\sigma'} = M_{yy}^{\sigma\sigma'}$  and the second order contributions to the energy shift  $\Delta$  is given by

$$\Delta_2 = \sum_{\sigma\sigma'} \sum_x M_{xx}^{\sigma\sigma'} S_x^{\sigma\sigma'} S_x^{\sigma'\sigma}. \quad (19)$$

Assuming the states  $(\mu_1, \mu_2) = (\uparrow, \downarrow)$  are chosen to be parallel to the  $z$  axis, the most general set of spinors are generated from the following unitary transformation

$$\begin{aligned} |\chi_1\rangle &= e^{i\gamma} \left[ \cos \frac{\theta}{2} |\uparrow\rangle + e^{i\beta} \sin \frac{\theta}{2} |\downarrow\rangle \right] \\ |\chi_2\rangle &= e^{-i\gamma} \left[ -e^{-i\beta} \sin \frac{\theta}{2} |\uparrow\rangle + \cos \frac{\theta}{2} |\downarrow\rangle \right], \end{aligned} \quad (20)$$

where  $\theta$  and  $\beta$  are variational parameters and  $\gamma$  is an ignorable parameter. After performing a bit of algebra the total second order shift  $\Delta_2$  becomes

$$\begin{aligned} \Delta_2 &= (M_{xx}^{11} + M_{xx}^{22} + M_{zz}^{12} + M_{zz}^{21}) \frac{\sin^2(\theta)}{4} \\ &+ (M_{zz}^{11} + M_{zz}^{22} + M_{xx}^{12} + M_{xx}^{21}) \frac{\cos^2(\theta)}{4} \\ &+ (M_{xx}^{12} + M_{xx}^{21}) \frac{1}{4} \\ &= A + \frac{\gamma}{2} \left[ \frac{\Delta N \cos \theta}{2} \right]^2 \end{aligned} \quad (21)$$

with  $A = (M_{xx}^{11} + M_{xx}^{22} + M_{zz}^{12} + M_{zz}^{21} + M_{xx}^{12} + M_{xx}^{21})/4$  and

$$\begin{aligned} \gamma &= (2/\Delta N^2) (M_{zz}^{11} + M_{zz}^{22} + M_{xx}^{12} + M_{xx}^{21} - M_{xx}^{11} \\ &- M_{xx}^{22} - M_{zz}^{12} - M_{zz}^{21}). \end{aligned}$$

In the above equation we have used the fact that for a uniaxial system,  $M_{xx}^{\sigma\sigma'} = M_{yy}^{\sigma\sigma'}$ . It is convenient to define  $\gamma$  in this way because  $\langle S_z \rangle = \Delta N \cos \theta/2$ . While this is formally a classical expectation value of a spin projection and a continuous function of  $\theta$ , it is clear that  $\langle S_z \rangle$  exhibits the appropriate bounds  $|\langle S_z \rangle| \leq \Delta N/2$ . The difference between the maximum energy orientation and the minimum energy orientation is given by  $(\Delta N^2/4)(\gamma/2)$ . A positive gamma corresponds to an easy plane (no barrier) and a negative gamma corresponds to an easy axis with a barrier at  $\langle S_z \rangle = 0$  and minima at  $\langle S_z \rangle = \pm \Delta N/2$ . It is the latter case that is of interest to spin tunneling experiments.

To make contact with spin tunneling experiments we now consider the case where the magnetic field is taken along the  $z$  axis. Combining Eqs. (16) and (21) leads to

$$\begin{aligned} \Delta &= A + \frac{B}{c} \frac{\Delta N \cos \theta}{2} + \frac{\gamma}{2} \left[ \frac{\Delta N \cos \theta}{2} \right]^2 \\ &= A + \frac{B}{c} \langle S_z \rangle + \frac{\gamma}{2} \langle S_z \rangle^2. \end{aligned} \quad (22)$$

Assuming  $\gamma$  is positive and equating the total azimuthal quantum number  $M_S = \langle S_z \rangle$  several different effects due to small magnetic fields can be experimentally observed. Most relevant to spin tunneling is to imagine preparing a collection of the molecules in a state  $M_S = S$  with the total spin  $S = \Delta N/2$ . Over a period of time the spin projections will reorientate and the relaxation time for redistribution is related to the classical barrier which is  $S^2(\gamma/2)$ . If one measures the relaxation time in the presence of a magnetic field the relaxation time changes because the barrier height changes continuously with field. However it is easily verified that for integer multiples of the field strength  $B_0 = \gamma c/2$ , states on one side of the barrier will be degenerate with states on the other side of the barrier. Under these conditions quantum tunneling of spins occurs which leads to discontinuities in the relaxation times. For a discussion of actual transition mechanisms see Ref. 19. For a perfectly quadratic system these discontinuities would provide a more accurate way of

measuring the parameter  $\gamma$  and, therefore, the classical energy barrier. Alternatively, deviations between the barriers determined from the Arrhenius law and those deduced by a harmonic analysis of the resonance field strengths provide a measure of the strength of the higher-order contributions to the anisotropy barriers.

#### IV. ELECTRONIC, MAGNETIC AND GEOMETRICAL STRUCTURE

The theoretical studies were carried out using a linear combination of Gaussian orbitals molecular orbital approach within the density functional formalism using the generalized gradient approximation<sup>20</sup> (GGA) of the density functional theory.<sup>21</sup> Discussion of this methodology (NRLMOL) has appeared elsewhere<sup>22</sup> and discussion specific to the  $\text{Mn}_{12}\text{O}_{12}$  core (e.g., basis sets) appears in Ref. 14. For the first iteration of the first geometry, we used a starting potential which favored the ferrimagnetic ordering suggested by experiment. After the first iteration and for all subsequent geometries, this external potential was removed and the Kohn-Sham orbitals and atomic positions were optimized to minimize the energy of the system. In accord with the experimental understanding, we found a ferrimagnetic structure which consists of an inner  $\text{Mn}_4\text{O}_4$  core of minority spin atoms and an outer  $\text{Mn}_8\text{O}_8$  ring of majority spin atoms. The cluster carries a net moment of  $S = 20\mu_B$  in agreement with experiment. We have calculated the moment captured by a sphere of radius 2.5 Bohr centered about each Mn atom and found local moments of  $-2.6$  and  $3.6\mu_B$  on the four inner and eight outer Mn atoms, respectively. While the magnetization density is not localized entirely on the Mn atoms, the simple experimental interpretation of four Mn atoms with moments of  $-3.0$  and eight Mn atoms with moments of  $4.0\mu_B$  is quite reasonable.

Since the Kohn-Sham orbitals contain the information that is required for determination of the tunneling barrier, we first discuss the electronic structure of the passivated  $\text{Mn}_{12}\text{O}_{12}$  molecule. For the passivated structure, the energies of the minority spin HOMO and lowest unoccupied molecular orbital (LUMO) levels are found to be  $-6.08$  and  $-4.00$  eV, respectively, while the majority spin HOMO and LUMO levels are found to be  $-4.89$  and  $-4.45$  eV, respectively. The passivated molecule approaches a half metallic *ferrimagnetic* system with a large minority-spin gap (2.08 eV) and a small majority-spin gap (0.45 eV), respectively. It would be nice if photoemission experiments on the crystal can be carried out to verify this feature. The majority-minority and minority-majority spin flip gaps (1.63 and 0.89 eV, respectively) are both positive which ensures that the system is stable with respect to the total magnetic moment. Pictured in Fig. 1 are plots of the relevant densities of states (DOS) for the majority and minority electronic states. For each spin the total densities of states is decomposed further into “inner and outer Mn 3d” contributions and the “oxygen 2p” contributions. The inner Mn 3d contributions correspond to the projection of the densities of states onto the Mn 3d states of the Mn atoms that form the inside cube. The outer 3d contributions correspond to a projection of the DOS onto the one of the eight Mn atoms which form the outer ring. The oxygen 2p contributions correspond to the projection onto the 2p states of the twelve core oxygen atoms

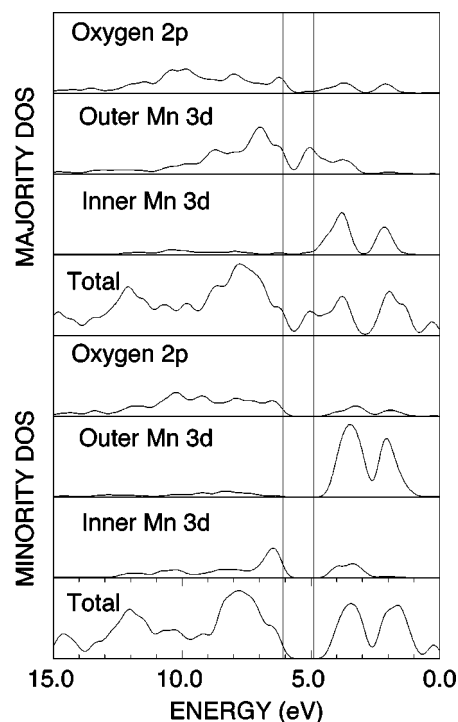


FIG. 1. Pictured above are the electronic densities of states (DOS), broadened by 0.54 eV of the  $\text{Mn}_{12}\text{O}_{12}(\text{HCOO})_{16}(\text{H}_2\text{O})_4$  molecule. For each spin, the total DOS, projected inner and outer Mn(3d) DOS, and projected O(2p) DOS of the 12 core O atoms are presented. The two vertical lines at  $-6.08$  and  $-4.89$  eV represent the energy of the highest occupied molecular orbitals (HOMO's) for each spin. Units are arbitrary, but the same scale has been used for all projected DOS plots.

pictured in Fig. 2. The projected Mn 3d densities of states clearly show that the system exhibits ferrimagnetic ordering. The minority spin valence electrons are composed of 3d electrons on the four inner Mn atoms while the majority spin valence electrons primarily reside on the outer ring. The projected densities of states for the O(2p) levels clearly show

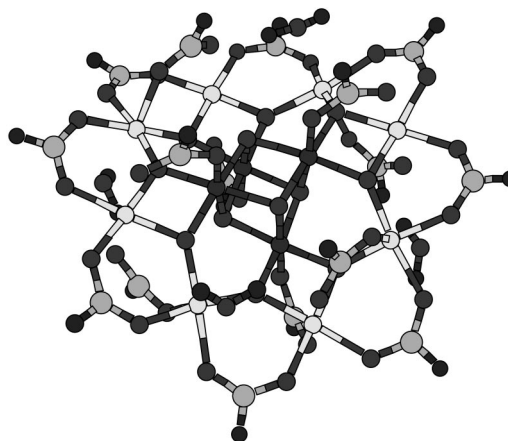


FIG. 2. Geometry of  $\text{Mn}_{12}\text{O}_{12}(\text{HCOO})_{16}(\text{H}_2\text{O})_4$  determined from NRLMOL. The four minority spin Mn atoms form a cube at the center of the molecule and the eight majority spin Mn from a puckered ring around the inner cube. The O atoms associated with the HCOO ligands and water molecules coordinate themselves with the Mn atoms so that each of the metal atoms is sixfold coordinated.

TABLE I. Magnetic anisotropy energy (barrier) as a function of cutoff energy  $E_{\text{cut}}$  (above  $\epsilon_F$ ) for truncation of unoccupied state summation [Eq. (2)]. Also included is the number of occupied and unoccupied states used in Eq. (2). The experimental data is from Ref. 13.

$E_{\text{cut}}$ (eV)	$N_{\text{occ}}$	$N_{\text{unocc}}$	Barrier (K)
6.8	804	381	55.8
13.6	804	730	55.7
27.2	804	1258	55.7
13.6 (valence only)	460	730	55.7
Experiment			55.6

that the interaction between the Mn and O states is not entirely ionic. In addition to ionic bonding, there is some degree of covalency and also some exchange coupling between the like-spin Mn( $3d$ ) and O( $2p$ ) states. The covalent bonding and exchange coupling are responsible for reducing the local Mn moments from  $\pm 4.2\mu_B$  in the isolated magnetic core<sup>14</sup> to  $-2.6$  and  $3.6\mu_B$  in the passivated structure.

In the energy region between the minority spin HOMO and the majority spin HOMO ( $-6.08$  to  $-4.89$  eV), there is a forbidden region for the minority spin electrons, but there is significant weight from the majority spin electrons. The projected densities of states show that these states are primarily associated with the outer eight Mn  $3d$  electrons, but some weight also appears in the O  $2p$  channels.

#### V. DENSITY-FUNCTIONAL-BASED DETERMINATION OF SPIN TUNNELING BARRIERS AND RESONANCE FIELDS: THE Mn-ACETATE MOLECULE

We now turn to a discussion and of our calculations on the anisotropy barrier for this molecule. In a previous paper<sup>15</sup> we showed that a simple electronic spin flip costs an energy of 0.90 eV (4900 K) which is large compare to the energy scale for the transitions observed in the spin tunneling experiments. We have calculated  $\gamma$  using the formalism discussed in Sec. III. As shown in Table I, our calculated value for the quadratic term gives a barrier of  $100(\gamma/2) = 55.7$  K in good agreement with the experimental Arrhenius results which finds a barrier in the range of 60–62 K. Of course the Arrhenius behavior samples the full barrier rather than the quadratic part of the barrier that we have calculated. Recently Barra *et al.* have analyzed electron paramagnetic resonance data and have determined both the quadratic and higher order contributions to the anisotropy energy. Their value of  $\gamma/2$  (referred to a  $\alpha$  in Ref. 12) is found to be 0.556 K. Thus the experimentally determined second order contributions to the anisotropy energies are 55.6 K in excellent agreement with our calculated value. We now turn to an analysis of the electronic states that form the barrier and a discussion of the convergence tests that we have performed in our calculations.

The excess majority spin electrons are very delocalized which facilitates their observation of the anisotropy of the molecule. Since they are also energetically closest to the Fermi level, one would generally expect that interactions between these states and unoccupied states close to the Fermi level would give the largest contributions to the anisotropy

barrier since the energy denominators in Eq. (18) are small. As discussed below we have ascertained that states within an 8.0 eV window of the Fermi level account for 98% of the anisotropy barrier. However, contrary to what is expected from considering energy denominators alone, our calculations show that it is the matrix elements between occupied *majority* spin electrons and unoccupied *minority* spin electrons that account for 65% of the second-order anisotropy barrier. The matrix elements between occupied minority-spin electrons and unoccupied majority-spin electrons account for 21% of the barrier. The smallest energy denominators in these sums are 0.89 and 1.63 eV, respectively, which is significantly larger than the smallest energy gap (majority-majority) of 0.45 eV in the problem. Even with this small gap, interactions between the majority occupied and majority unoccupied electrons contribute only 13% to the anisotropy barrier. The interactions between the minority unoccupied and minority occupied electrons, for which the smallest energy denominator is 2.08 eV, contribute only 1% to the anisotropy barrier. This analysis shows that while energy denominators are important it is spatial overlap between occupied and unoccupied states of different spins that are most important for enhancing the anisotropy barrier in the Mn-acetate molecule. To increase the size of the barrier one would want to concentrate on further enhancing the spatial overlap of the majority occupied and minority unoccupied electrons or decreasing the energy denominators between these states.

We now show that our results are converged with respect to the number of occupied and unoccupied electrons used in the perturbative expansion [Eq. (18)]. The results are presented in Table I. For the first three lines of Table I, we have used all of the occupied states and a variable number of unoccupied states that are within 6.8, 13.6, and 27.2 eV of the Fermi level. For the last line we have neglected the core electrons in the summation over occupied orbitals and used a 13.6 eV cutoff for the unoccupied state summation. Finally, we report that if we only include the occupied and unoccupied electrons that are within 8.0 eV window of the Fermi level (160 occupied and 116 unoccupied electrons) we find an anisotropy energy of 54.7 K which is close to our converged value. This shows that it is indeed the delocalized majority spin valence states that are most important for determining the tunneling barriers.

#### VI. SUMMARY

In summary, we have shown that the building block of the Mn-acetate molecule is intrinsically ferrimagnetic with an electronic density of states that approaches a half-metallic ferrimagnetic behavior. The moments on the Mn atoms and the overall stability of the molecule is significantly impacted by the presence of the carboxyl groups. We have used a new computational strategy to perform a calculation of the spin-tunneling barrier for this molecule which manifests itself due to spin-orbit coupling. Our results are in excellent agreement with experiment and show that the coupling between the majority-spin valence and minority-spin conduction are primarily responsible for the second order anisotropy barrier. We suggest that pressure-dependent experiments which change the shape of the electronic wave functions and the

band gaps could be used to control the anisotropy barriers.

While less important in uniaxial systems, higher order corrections to anisotropy barriers are believed to require the inclusion of the Breit-Darwin interaction (See Refs. 1,2). However, the simplified Cartesian representation introduced here will accurately describe all collective effects that arise from the spin-orbit interaction and the Hartree potential. The Cartesian representation is more convenient than the standard  $\mathbf{L}\cdot\mathbf{S}$  representation because it does not require the evaluation of electric fields and there is no explicit depen-

dence on the atomic positions. While implemented within perturbation theory here, a complete variational treatment is also easily achievable.

#### ACKNOWLEDGMENTS

S.N.K. is grateful to the U.S. Department of Energy (Grant No. DE-FG02-96ER45579) for financial support. M.R.P. was supported in part by the ONR Molecular Design Institute (Grant No. N0001498WX20709).

- 
- <sup>1</sup>J. Van Vleck, Phys. Rev. **52**, 1178 (1937).  
<sup>2</sup>For early discussions of the electronic-structure based calculation of magnetic anisotropies in metals, see H.J.F. Jansen, Phys. Rev. B **38**, 8022 (1988).  
<sup>3</sup>T. Lis, Acta Crystallogr., Sect. B: Struct. Crystallogr. Cryst. Chem. **36**, 2042 (1980).  
<sup>4</sup>J.R. Friedman, M.P. Sarachik, J. Tejada, and R. Ziolo, Phys. Rev. Lett. **76**, 3830 (1996).  
<sup>5</sup>L. Thomas, F. Lioni, R. Ballou, D. Gatteschi, R. Sessoli, and B. Barbara, Nature (London) **383**, 145 (1996).  
<sup>6</sup>A. Caneschi, D. Gatteschi, and R. Sessoli, J. Am. Chem. Soc. **113**, 5873 (1991).  
<sup>7</sup>R. Sessoli, H.-L. Tsai, A.R. Schake, S. Wang, J.B. Vincent, K. Folting, D. Gatteschi, G. Christou, and D.N. Hendrickson, J. Am. Chem. Soc. **115**, 1804 (1993).  
<sup>8</sup>R. Sessoli, D. Gatteschi, A. Caneschi, and M.A. Novak, Nature (London) **365**, 141 (1993).  
<sup>9</sup>J. Hernandez, X. Zhang, F. Louis, J. Bartolome, J. Tejada, and R. Ziolo, Europhys. Lett. **35**, 301 (1996).  
<sup>10</sup>J. Villain, F. Hartman-Boutron, R. Sessoli, and A. Rettori, Europhys. Lett. **27**, 159 (1994).  
<sup>11</sup>F. Fominaya, J. Villain, P. Gandit, J. Chaussy, and A. Caneschi, Phys. Rev. Lett. **79**, 1126 (1997).  
<sup>12</sup>A.L. Barra, D. Gatteschi, and R. Sessoli, Phys. Rev. B **56**, 8192 (1997).  
<sup>13</sup>A. Fort, A. Rettori, J. Villain, D. Gatteschi, and R. Sessoli, Phys. Rev. Lett. **80**, 612 (1998).  
<sup>14</sup>M.R. Pederson and S.N. Khanna, Phys. Rev. B **59**, R693 (1999).  
<sup>15</sup>M. R. Pederson and S. N. Khanna, Chem. Phys. Lett. **303**, 373 (1999).  
<sup>16</sup>P.J. Ziemann and A.W. Castleman, Jr., Phys. Rev. B **46**, 13 480 (1992).  
<sup>17</sup>For example, see S. Gasiorowicz, *Quantum Physics* (Wiley, New York, 1974), p. 272.  
<sup>18</sup>C. Kittel, *Introduction to Solid State Physics* (Wiley, New York, 1963), p. 181.  
<sup>19</sup>E.M. Chudnovsky and L. Gunther, Phys. Rev. Lett. **60**, 661 (1988).  
<sup>20</sup>J.P. Perdew, K. Burke, and M. Ernzerhof, Phys. Rev. Lett. **77**, 3865 (1996).  
<sup>21</sup>W. Kohn and L.J. Sham, Phys. Rev. **140**, A1133 (1965).  
<sup>22</sup>M.R. Pederson and K.A. Jackson, Phys. Rev. B **41**, 7453 (1990); K.A. Jackson and M.R. Pederson, *ibid.* **42**, 3276 (1990); D. V. Porezag, Ph.D. thesis, Chemnitz Technical Institute, 1997.